



# Unravelling long-term source removal effects and chlorinated methanes natural attenuation processes by C and Cl stable isotopic patterns at a complex field site

Diana Rodríguez-Fernández <sup>a,\*</sup>, Clara Torrentó <sup>a,b</sup>, Jordi Palau <sup>a,b,c</sup>, Massimo Marchesi <sup>a,d</sup>, Albert Soler <sup>a</sup>, Daniel Hunkeler <sup>b</sup>, Cristina Domènech <sup>a</sup>, Mònica Rosell <sup>a</sup>

<sup>a</sup> Grup MAiMA, Mineralogia Aplicada, Geoquímica i Geomicrobiologia, Departament de Mineralogia, Petrologia i Geologia Aplicada, Facultat de Ciències de la Terra, Universitat de Barcelona (UB), C/Martí i Franquès s/n, 08028 Barcelona, Spain

<sup>b</sup> Centre for Hydrogeology and Geothermics, University of Neuchâtel, 2000 Neuchâtel, Switzerland

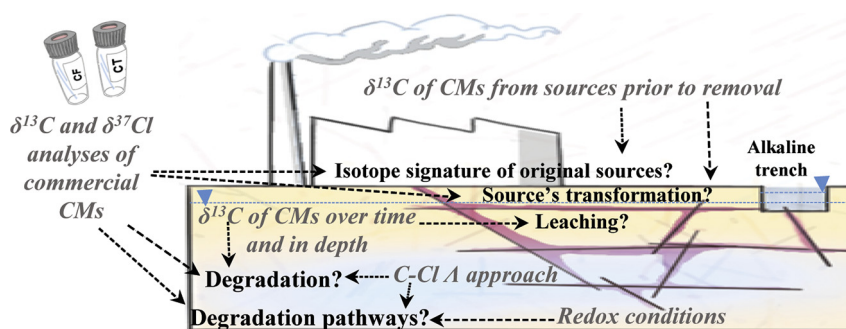
<sup>c</sup> Institute of Environmental Assessment and Water Research (IDAEA), CSIC, Jordi Girona 18-26, 08034 Barcelona, Spain; Associated Unit: Hydrogeology Group (UPC-CSIC), Barcelona, Spain

<sup>d</sup> Politecnico di Milano, Dept. of Civil and Environmental Engineering (DICA), Piazza L. Da Vinci, 32, 20133 Milano, Italy

## HIGHLIGHTS

- Long-term  $\delta^{13}\text{C}$  monitoring of chlorinated methanes (CMs) after source removal.
- CMs concentration and  $\delta^{13}\text{C}$  study enabled detection of still active CMs sources.
- Assessment of CT and CF field degradation processes by dual C-Cl isotope approach.
- CF oxidation or/and alkaline hydrolysis in pit and CT reduction in tank zone.
- CT thiolytic reduction in wastewater pipe is combined with hydrogenolysis.

## GRAPHICAL ABSTRACT



## ARTICLE INFO

### Article history:

Received 7 May 2018

Received in revised form 10 July 2018

Accepted 10 July 2018

Available online xxx

Editor: Frederic Coulon

### Keywords:

Carbon tetrachloride

Chloroform

2D-CSIA

Case study

Ódena site

## ABSTRACT

The effects of contaminant sources removal in 2005 (i.e. barrels, tank, pit and wastewater pipe sources) on carbon tetrachloride (CT) and chloroform (CF) concentration in groundwater were assessed at several areas of a fractured multi-contaminant aquifer (Ódena, Spain) over a long-term period (2010–2014). Changes in redox conditions, in these chlorinated methanes (CMs) concentration and in their carbon isotopic compositions ( $\delta^{13}\text{C}$ ) were monitored in multilevel wells.  $\delta^{13}\text{C}$  values from these wells were compared to those obtained from sources (barrels, tank and pit before their removal, 2002–2005) and to commercial solvents values in literature. Additionally, CMs natural attenuation processes were identified by C-Cl isotope slopes ( $\Lambda$ ).

Analyses revealed the downstream migration of the pollutant focus and an efficient removal of DNAPLs in the pit source's influence area. However, the removal of the contaminated soil from former tank and wastewater pipe was incomplete as leaching from unsaturated zone was proved, evidencing these areas are still active sources. Nevertheless, significant CMs degradation was detected close to all sources and  $\Lambda$  values pointed to different reactions. For CT in the tank area,  $\Lambda$  value fitted with hydrogenolysis pathway although other possible reduction processes were also uncovered. Near the wastewater pipe area, CT thiolytic reduction combined with hydrogenolysis was derived. The highest CT degradation extent accounted for these areas was  $72 \pm 11\%$  and  $84 \pm 6\%$ , respectively. For CF, the  $\Lambda$  value in the pit source's area was consistent with oxidation and/or with transport of CF affected by alkaline hydrolysis from upstream interception trenches. In contrast, isotope data

\* Corresponding author.

E-mail address: [diana.rodriguez@ub.edu](mailto:diana.rodriguez@ub.edu) (D. Rodríguez-Fernández).

evidenced CF reduction in the tank and wastewater pipe influence areas, although the observed  $\Lambda$  slightly deviates from the reference values, likely due to the continuous leaching of CF degraded in the non-saturated zone by a mechanism different from reduction.

© 2018 Elsevier B.V. All rights reserved.

## 1. Introduction

Carbon tetrachloride (CT) and chloroform (CF) are volatile organic compounds (VOCs) from the chlorinated methanes (CMs) group, considered toxic pollutants by the USEPA (2014). Identifying sources and tracing their evolution over time is crucial to set up effective decontamination strategies (Penny et al., 2010; Cappelletti et al., 2012).

In groundwater, CT degradation only occurs under anoxic conditions. CT can be reduced biotically or by Fe(II) sorbed on iron oxy/hydroxides surfaces to CF and then to dichloromethane (DCM) following a hydrogenolysis pathway. In addition, CT “hydrolytic reduction” (e.g. by magnetite) initiates with a reduction and leads, after different steps including hydrolysis, to formate, CO and CO<sub>2</sub> as final products. CT “thiolitic reduction”, after an initial reduction, produces CS<sub>2</sub> as final product by thiolitic substitution of dechlorinated intermediates, being mediated either by Fe(II)-sulfides or by bacteria (Field and Sierra-Alvarez, 2004; Penny et al., 2010; Koenig et al., 2012; He et al., 2015). CT reduction by *Pseudomonas stutzeri* also produces CO<sub>2</sub> as the final product, with transient accumulation of toxic phosgene and thiophosgene (Lewis and Crawford, 1995).

CF degradation occurs under oxic and anoxic conditions. Under oxic conditions, cometabolic microbial reactions transform CF to CO<sub>2</sub> (Cappelletti et al., 2012). Abiotic reactions like oxidation (e.g. by persulfate) and CF alkaline hydrolysis have been proved as efficient CF remediation strategies (Torrentó et al., 2014, 2017). Under anoxic conditions, direct or indirect “hydrolytic reduction” of CF and cometabolic hydrogenolysis are described, the latter being associated to methanogens, fermenting bacteria and sulfate reducers (Cappelletti et al., 2012). Finally, *Dehalobacter* and *Desulfitobacterium* genera are able to dechlorinate CF to DCM by organohalide respiration (Groster et al., 2010; Chan et al., 2012; Lee et al., 2012; Deshpande et al., 2013; Tang and Edwards, 2013; Ding et al., 2014).

CT and CF inhibit mutual biodegradation (Groster et al., 2010; Lima and Sleep, 2010; Justicia-Leon et al., 2014) and also microbial respiration of chlorinated ethanes and ethenes by *Dehalococcoides* and *Desulfitobacterium* species (Bagley et al., 2000; Weathers and Parkin, 2000; Maymó-Gatell et al., 2001; Duhamel et al., 2002; Futagami et al., 2006, 2013), and this hinders natural attenuation and bioremediation strategies in complex sites impacted by mixtures of chlorinated compounds.

According to the European Environment Agency (EEA, 2014), ex situ physical and/or chemical treatments represent 37% of the techniques used in groundwater decontamination. Monitored Natural Attenuation (MNA) is an alternative cost-effective treatment, although it requires appropriate quantification and evaluation over time (Wiegert et al., 2012). There are only few MNA case studies of CT and CF in polluted sites, mainly based on the detection and quantification of by-products (Devlin and Muller, 1999; Davis et al., 2003; Puigserver et al., 2013). However, monitoring parental and by-product compounds concentration as an indicator of (bio)degradation has some limitations, such as i) long periods of time are often necessary to detect a significant decrease in concentrations, especially at highly polluted sites or when sources have not been removed; ii) no clear conclusions can be drawn when a given compound appears as both parent and by-product; when a by-product originates from multiple parent compounds; or when the target by-product is further degraded and iii) sorption or desorption, differential transport or dilution events could also produce concentrations variations but not degradation.

To overcome these limitations, compound specific isotope analysis (CSIA) is increasingly used for source apportionment and in situ assessment of chlorinated ethenes and ethanes MNA (Wiegert et al., 2012, 2013; Kuder et al., 2013; Badin et al., 2014, 2016; Kaown et al., 2014; Palau et al., 2014, 2016; Audí-Miró et al., 2015). Moreover, dual isotopic studies (2D-CSIA) with carbon and chlorine isotope analyses have allowed more precise identification of pollutants' origin and fate as dual isotope slopes ( $\Lambda$ ) reflect ongoing degradation mechanisms and can be compared with characteristic slopes from laboratory studied reactions (Hunkeler et al., 2009). However, an aged source of contamination would have undergone fractionation processes in the unsaturated zone distinctly or not to those occurred in the saturated zone (Jeannotat and Hunkeler, 2012, 2013) and, thus, it would hamper reliable degradation processes discrimination. Therefore, if the original pure phase is not available, the study and comparison of isotope values from wells respect to the ones located in source areas (Wiegert et al., 2012) or to the known range of commercial solvents values (Holt et al., 1997; Jendrzewski et al., 2001; Shouakar-Stash et al., 2003) is strongly advisable (Imfeld et al., 2008; Palau et al., 2014). To our knowledge, there are only few field CSIA studies dedicated to CMs. These studies are mainly based on carbon isotope measurements to confirm CT degradation in the non-saturated zone (Kirtland et al., 2003), to characterize the very depleted  $\delta^{13}\text{C}$  of CT and CF industrially produced from methane (Nijenhuis et al., 2013), to confirm CF degradation, along with concentration data, in a multi-contaminant polluted aquifer (Hunkeler et al., 2005) and/or to evaluate CF remediation treatment by alkaline hydrolysis in Òdena site (NE Spain) (Torrentó et al., 2014). New methods for chlorine isotope analyses of CMs and reference  $\Lambda$  values have only become available recently (Heckel et al., 2017a, 2017b; Torrentó et al., 2017; Rodríguez-Fernández et al., 2018a, 2018b). Thus, there are not previous field site studies testing 2D-CSIA approach potential to identify CMs degradation pathways in complex fractured systems with multi-contaminant spills like that of Òdena. These aquifer features increases the difficulty of pollutant monitoring and the need of CSIA techniques to control the contaminant plume.

The first goal of this research consisted in identifying potential aging of these sources and uncovering CMs active leaching sources by using C-CSIA and comparing CMs isotope values from sources before their removal at the Òdena site (NE Spain) with those of CMs commercial solvents and of groundwater samples. The second goal was to unravel the long-term effect of the pollutant sources removal in CMs behaviour and to detect the occurrence of CMs natural attenuation processes. For that end, CMs degradation by-products,  $\delta^{13}\text{C}$  shifts and redox values were monitored over time. Finally, the third goal was to evaluate 2D-CSIA approach potential to identify CMs degradation pathways in a complex fractured aquifer. To this end, dual C-Cl isotope plots of the different multilevel wells were compared with data from literature and from recent microcosms studies performed with Òdena site slurry (Rodríguez-Fernández et al., 2018a).

## 2. Material and methods

### 2.1. Site description

The studied site is an unconfined bedrock aquifer located in Òdena (NE Spain) (Palau et al., 2014; Torrentó et al., 2014). The aquifer is mainly composed of low permeability fractured limestone. The groundwater is polluted with a mixture of pollutants ranging from chlorinated

aliphatic hydrocarbons and chlorobenzenes to pesticides and BTEXs. Groundwater pollution was attributed to three main potential contaminant sources (i.e., barrels with solvents, a pit and a tank where wastewater was spilled) of a former chemical plant working from 1978 to 1985 (Fig. 1), although some other spills were detected and mentioned as potential chlorinated ethenes contamination sources (Palau et al., 2014). CT, CF and DCM were found as pure phase solvents in the barrels abandoned in the industrial plant. In 2005, contaminated soil of the tank and pit areas was removed (Palau et al., 2014; Torrentó et al., 2014) and the barrels and the wastewater pipe system were dismantled. The tank and pit excavated areas in the non-saturated zone (hereafter called trenches) were filled with concrete-based construction wastes aiming to induce alkaline conditions (pH ~12) and, thus, promote CF degradation through alkaline hydrolysis (Torrentó et al., 2014).

## 2.2. Sample collection

During the 2002–2005 period, before the removal of the sources, liquid samples were taken with a bailer from the barrels and tank as well as water samples, from pit area (Palau et al., 2014) for CT, CF and DCM concentration and  $\delta^{13}\text{C}$  analyses. In June 2006, June 2007, September 2007, January 2008, March and November 2010 (Mar-10 and Nov-10 hereafter), March 2013 (Mar-13) and November 2014 (Nov-14) water samples from 8 multilevel wells (S1, S3, S4, S6, S7, S8, S9 and S10, Fig. 1) were taken using flexible polytetrafluoroethylene (PTFE) tubes and disposable 60 mL polypropylene sterile syringes for pH and Eh measurements, total Ca, Na, Fe,  $\text{Cl}^-$ ,  $\text{HCO}_3^-$ ,  $\text{NO}_3^-$  and  $\text{SO}_4^{2-}$  and VOCs concentration analyses as well as isotopic analyses.  $\delta^{34}\text{S}$  and  $\delta^{18}\text{O}$  analyses of dissolved sulfate were done in June 2006 and Mar-13 campaigns. In Mar-10, Nov-10, Mar-13 and Nov-14 VOCs concentration and  $\delta^{13}\text{C}$  measurements were also done.  $\delta^{37}\text{Cl}$  measurements were only performed in Mar-13 for CF and in Nov-14 for CT and CF. In addition, different commercial CT, CF and DCM solvents were analysed to complete the range of  $\delta^{13}\text{C}$  and  $\delta^{37}\text{Cl}$  reported in the literature for CMs (see Table A2 in

supplementary information, SI, for commercial solvent details). All samples were stored until analysis in sterile amber glass bottles, completely filled and closed with PTFE-lined caps.

## 2.3. Analytical methods

pH and Eh were monitored in field samples using a pH-meter (Crison 6037) and a redox sensor (SenTix® ORP 900), respectively. Aliquots of samples were preserved with nitric acid to measure total concentrations of Fe, Ca and Na by inductively coupled plasma-optical emission spectrometry (ICP-OES, Optima 3200 RL) and by inductively coupled plasma-mass spectrometry (ICP-MS, Elan 6000) at the *Centres Científics i Tecnològics de la Universitat de Barcelona* (CCiT-UB).  $\text{HCO}_3^-$  was determined by titration (METROHM 702SM Titrino).  $\text{NO}_3^-$ ,  $\text{Cl}^-$  and  $\text{SO}_4^{2-}$  concentrations were analysed by high-performance liquid chromatography (HPLC) using a WATERS 515 HPLC pump with an IC-PAC anion column and a WATERS detector (mod 432) at the CCiT-UB. To identify the predominant equilibrium system controlling the Eh, Eh-pH predominance diagrams were drawn with the MEDUSA code (Puigdomènech, 2010).

VOCs concentration measurements were done by headspace (HS) - gas chromatography (GC) - mass spectrometry (MS) at the CCiT-UB (Torrentó et al., 2014). The uncertainty based on replicate measurements was below 10% for all the compounds.

For the  $\text{SO}_4^{2-}$  isotopic analysis, the dissolved  $\text{SO}_4^{2-}$  was precipitated as  $\text{BaSO}_4$  according to (Dogramaci et al., 2001).  $\delta^{34}\text{S}$ - $\text{SO}_4^{2-}$  and  $\delta^{18}\text{O}$ - $\text{SO}_4^{2-}$  were analysed at the CCiT-UB as performed by Puig et al. (2013), except that a Finnigan Delta XP Plus IRMS was used for  $\delta^{34}\text{S}$  determination. Notation is expressed in terms of  $\delta$  (‰) relative to the international standard VSMOW (Vienna Standard Mean Oceanic Water) for  $\delta^{18}\text{O}$  and VCDT (Vienna Canyon Diablo Troilite) for  $\delta^{34}\text{S}$ . The reproducibility ( $1\sigma$ ) of the samples was  $\pm 0.2\%$  for  $\delta^{34}\text{S}$ - $\text{SO}_4^{2-}$  and  $\pm 0.5\%$  for  $\delta^{18}\text{O}$ - $\text{SO}_4^{2-}$ .

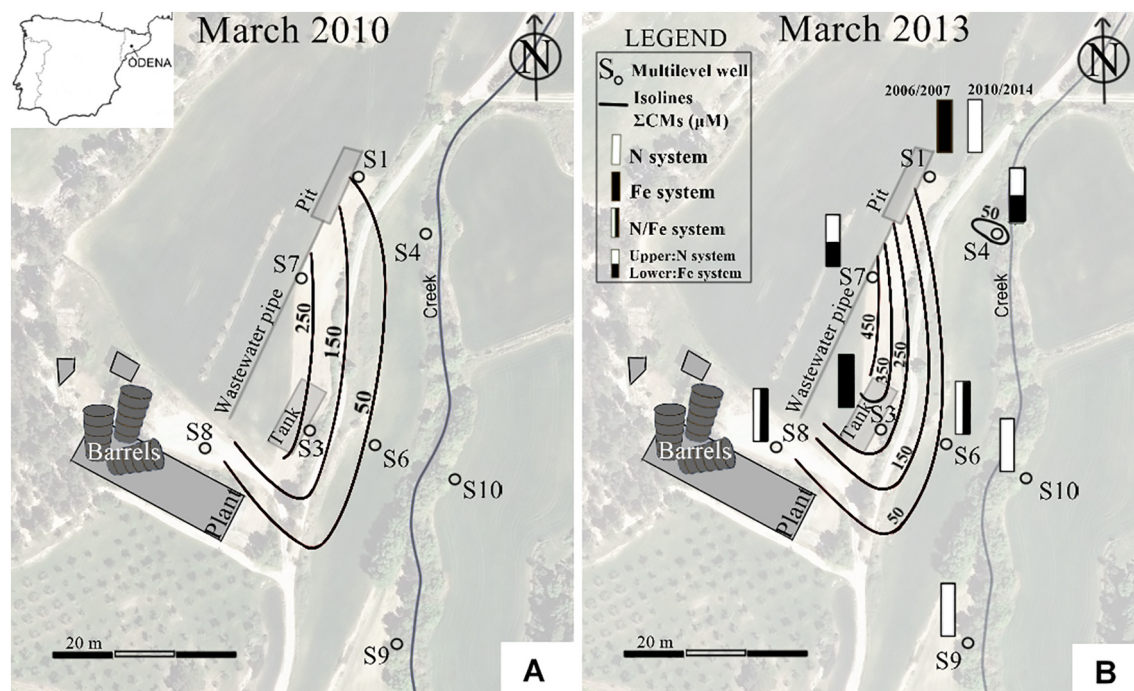


**Fig. 1.** Odena site map and groundwater monitoring wells network (S1–10). Groundwater flow system from Palau et al. (2014) was used to draw a simplified contamination CMs plume evolution (sum of molar concentrations of CT, CF and DCM at the most contaminated level for each well) from A) March 2010 to B) March 2013. The barrels from chemical plant, the tank, pit and the wastewater pipe were all removed in 2005 but are shown in the map for a better understanding. Rectangles in B represent the well's Eh-controlling system from 2006 to 2014, determined after analysing the Eh-pH diagrams (Fig. A1), calculated with data from field samples over time (Table A1). N system means equilibrium between nitrogen (N) chemical species of the N-H<sub>2</sub>O system and Fe system, equilibrium between iron (Fe) chemical species of the Fe-S-C-H<sub>2</sub>O system, according to Eh and pH values measured in each well. If changes in the redox conditions of a well were detected in Eh-pH diagrams (Fig. A1) in depth (i.e. S4 and S7) or over time (i.e. S1) they are also specified in the figure.

Carbon isotope analyses of CMs ( $\delta^{13}\text{C}_{\text{CT}}$ ,  $\delta^{13}\text{C}_{\text{CF}}$  and  $\delta^{13}\text{C}_{\text{DCM}}$ ) were also performed at the CCIT-UB by headspace (HS)-solid phase microextraction (HS-SPME) coupled to GC-isotope ratio mass spectrometry (IRMS) (Torrentó et al., 2014; Martín-González et al., 2015). Notation is expressed in terms of  $\delta$  (‰) relative to VPDB (Vienna Pee Dee Belemnite). Total instrumental uncertainty ( $2\sigma$ ) was considered as the standard deviation of duplicate measurements.

CT and CF chlorine isotope analyses ( $\delta^{37}\text{Cl}_{\text{CT}}$  and  $\delta^{37}\text{Cl}_{\text{CF}}$ ) were performed by HS-GC- quadrupole mass spectrometry (qMS) at the University of Neuchâtel (Heckel et al., 2017b). The averaged  $\delta^{37}\text{Cl}$  values were determined on the basis of ten injections of the same sample corrected by two-point calibration with known working standards interspersed along the sequence. Notation is expressed in terms of  $\delta$  (‰) relative to VSMOC (Vienna Standard Mean Oceanic Chlorine). The analytical uncertainty ( $2\sigma$ ) of  $\delta^{37}\text{Cl}$  measurements was in all cases below  $\pm 0.5\%$  ( $n = 10$  per sample).  $\delta^{37}\text{Cl}_{\text{CF}}$  measurements were only performed for the samples collected on Mar-13 and Nov-14 and  $\delta^{37}\text{Cl}_{\text{CT}}$  for those obtained on Nov-14.

Further details related to the above-mentioned methodologies are included in the SI.

For all these isotopic measurements, several international and laboratory standards have been interspersed among the analytical batches for normalization of analyses according to Coplen (2011).

For a given compound, the extent of degradation ( $D$ , %) was estimated following Eq. (1), derived from the Rayleigh distillation equation, where  $\epsilon\text{C}$  is the carbon isotopic fractionation of the selected degradation pathway and  $\delta^{13}\text{C}_t$  and  $\delta^{13}\text{C}_0$  are, respectively, the most positive value and the assumed to be the most similar to the original value found in the field site.

$$D (\%) = \left[ 1 - \left( \frac{\delta^{13}\text{C}_t + 1000}{\delta^{13}\text{C}_0 + 1000} \right)^{\frac{1000}{\epsilon\text{C}}} \right] \times 100 \quad (1)$$

Changes in both carbon and chlorine isotope values in the field should be  $>2\%$  so that the degradation is considered significant (Hunkeler et al., 2008; Bernstein et al., 2011).

### 3. Results and discussion

Due to the complexity of the Òdena site, the first results presented and discussed are those related to the CMs isotope data of the polluted sources (Subsection 3.1). Once sources are characterized, the evolution of CMs (and by-products) concentration and isotope data in the wells, as well as the occurrence of natural attenuation processes are discussed (Subsection 3.2). Finally, discussion focuses on the identification of the specific degradation pathways occurring at the site (Subsection 3.3).

#### 3.1. $\delta^{13}\text{C}$ data of CMs in sources prior to their removal

In this subsection,  $\delta^{13}\text{C}$  values of samples from the tank, pit and barrels sources (Table 1) are compared among them and with available commercial  $\delta^{13}\text{C}$  values (Table A2) in order to characterize them for

further multilevel wells data interpretation and to detect if some processes could have affected the sources.

$\delta^{13}\text{C}_{\text{CT}}$  values were only available for the tank source. They shifted from  $-16.1 \pm 0.9\%$  in 2003 to  $-11.31 \pm 0.04\%$  in 2004 (Table 1) and were well above the range of available commercial CT ( $-54.4$  to  $-37.0\%$ ) (Table A2).

Regarding CF, the  $\delta^{13}\text{C}_{\text{CF}}$  value of the barrels source ( $-46.2 \pm 0.4\%$ ) was within the range of commercial CF ( $-63.7$  to  $-43.2\%$ ) (Table 1). However, the  $\delta^{13}\text{C}_{\text{CF}}$  values of the tank and pit sources were more enriched than those from the barrels and commercial CF (Table 1). Thus, as  $\delta^{13}\text{C}_{\text{CF}}$  values of the tank and pit sources are not depleted in  $^{13}\text{C}$  with respect to the barrels, significant volatilization processes from neat volume of CMs coming from abandoned barrels can be discarded (Baertschi et al., 1953; Hunkeler and Aravena, 2000).

The  $\delta^{13}\text{C}_{\text{DCM}}$  in the tank ( $-36 \pm 3\%$ ) was also enriched relative to that of the barrels ( $-42.1 \pm 0.5\%$ ), although in this case both values are within or very close to the upper limit of available commercial DCM range (Table 1).

Therefore, results suggest that CMs normal fractionation processes started during the industrial process and/or once they were spilled in the tank and pit sources in some point between the industrial activity period (1978–1985) and 2003 (first tank source sampling), especially for CT. Thus, because of this, isotope information from these aged sources should be taken with caution as their CMs isotopic signature might not be representative of the original solvent spilled in the unsaturated zone that migrated downwards through the fractured limestone reaching the aquifer.

#### 3.2. Source removal effects and evidence of CT and CF natural attenuation

Given that the sources sampled between 2002 and 2005 were already aged, the  $\delta^{13}\text{C}$  values representative of original CMs sources, needed for assessing the long-term effect of the source's removal on CMs natural attenuation, were searched in those wells located in sources' influence areas. As suggested by groundwater flow paths (Palau et al., 2014) (Fig. 1), groundwater samples from wells S1 and S4 and wells S3 and S6 were selected as representative of the pit and tank source's influence areas, respectively. Wells S8 and S7 (Fig. 1) were considered as representative of zones vulnerable to pollution around the industrial plant building (where the barrels were found) and around the wastewater pipe circuit, respectively.

On the other hand, wells S9 and S10, respectively located further downstream and on the other side of the creek (Fig. 1), were studied as overall outer controls of the contaminated site.

##### 3.2.1. Pit source's influence area

In S1 well, located exactly in the former pit source (Fig. 1), the most abundant CM was CF in all campaigns (up to 97% out of total molar CMs concentration) (Fig. 2). Total CMs concentration decreased with time at all depths with no significant variation in CMs distribution with depth (Fig. 2). The CT content decreased by nearly one order of magnitude between Mar-10 and Nov-14 and DCM and  $\text{CS}_2$  were always  $<0.2 \mu\text{M}$  (Table A3).

**Table 1**

CT, CF and DCM carbon isotopic composition ( $\delta^{13}\text{C}$ , ‰) of the three Òdena site's pollution sources previously identified by Palau et al. (2014) are shown. Samples from the abandoned barrels, the tank and the pit were taken from 2002 to 2005.  $\delta^{13}\text{C}$  ranges of commercial CMs from different suppliers (see Table A2 in SI for details) are also shown. b.d.l.: below detection limit.

Compound	$\delta^{13}\text{C}$ (‰)	Barrels (2002)	Tank	Pit (2005)	Commercial CMs
			(2003)	(2004)	
CT		b.d.l.	$-16.1 \pm 0.9$	$-11.30 \pm 0.04$	$-54.4$ to $-37.0$
CF		$-46.2 \pm 0.4$	$-29.9 \pm 0.1$	$-34.0 \pm 0.6$	$-63.7$ to $-43.2$
DCM		$-42.1 \pm 0.5$	$-36 \pm 3$	b.d.l.	$-40.9$ to $-34.2$

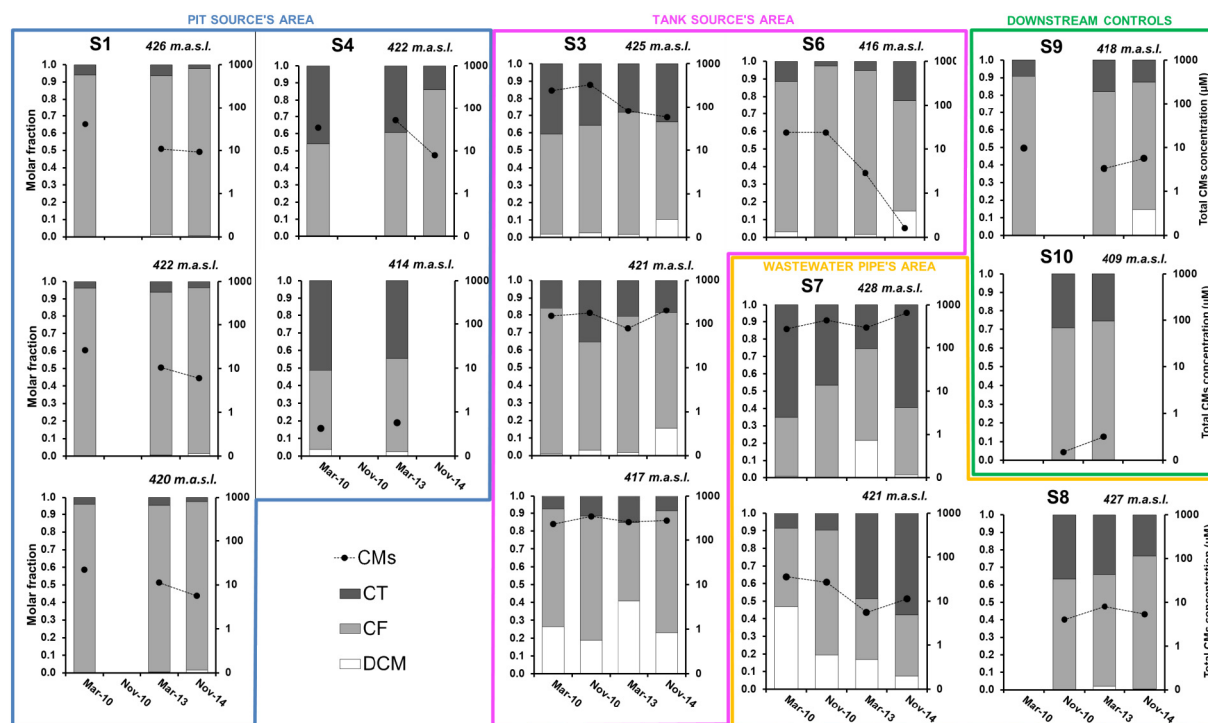


**Fig. 2.** Total CMs molar concentration ( $\mu\text{M}$ , dots), in logarithmic scale, and molar fraction distribution (bars) for Mar-10, Nov-10, Mar-13 and Nov-14 campaigns in wells S1, S4, S3, S7, S6, S8, S9 and S10. The panels are organized by clustering those wells belonging to a source's influence area (blue: pit source's area; fuchsia: tank source's area and orange: wastewater pipe area). S9 and S10 are the downstream controls in green. Different sampling depths for each well are represented when possible (in meters above sea level, m.a.s.l.). (For interpretation of the references to colour in this figure legend, the reader is referred to the web version of this article.)

Due to low concentrations,  $\delta^{13}\text{C}_{\text{CT}}$  values were only measured twice in S1 (Fig. 3A), being the value of Mar-10 ( $-30.0 \pm 0.5\%$ ) the most depleted value observed for CT within all sampling wells and campaigns. This  $\delta^{13}\text{C}_{\text{CT}}$  value is 20% lighter than the most enriched  $\delta^{13}\text{C}_{\text{CT}}$  value found in the site (from S3, Fig. 3C) and also more depleted than the values measured in the tank source (Table 1), which, in turn, was already considered degraded. Thus, the  $\delta^{13}\text{C}_{\text{CT}}$  value from S1 ( $-30.0 \pm 0.5\%$ ) had reached the aquifer before being significantly degraded in the unsaturated zone. Therefore, the  $\delta^{13}\text{C}_{\text{CT}}$  value from Mar-10 in S1 is more representative of the original CT than those values measured in the tank source between 2003 and 2004 (Table 1). This conclusion is also supported by a difference below 2‰ among the most depleted  $\delta^{13}\text{C}_{\text{CT}}$  values in S1, S4 and S8 wells (Fig. 3E), being the latter located near the industrial plant and upstream of any remediation action (Fig. 1).

In S1,  $\delta^{13}\text{C}_{\text{CF}}$  values in Mar-10 ( $-33 \pm 2$  and  $-32.8 \pm 0.3\%$ ) were slightly more enriched than those from the pit source and much more than those from the barrels or available commercial CF (Fig. 3B), evidencing CF fractionation processes. Over time,  $\delta^{13}\text{C}_{\text{CF}}$  values increased at all depths. This, in agreement with the decrease in CMs concentration (Fig. 2), suggests either CF in situ degradation or arrival of CF degraded by alkaline hydrolysis from the upstream trench (Torrentó et al., 2014). In contrast,  $\delta^{37}\text{Cl}_{\text{CF}}$  remained almost constant between Mar-13 ( $-3.8 \pm 0.5\%$  on average) and Nov-14 ( $-3.5 \pm 0.3\%$  on average) (Fig. 3B). These values, which are within the available range for commercial CF, were the most depleted  $\delta^{37}\text{Cl}_{\text{CF}}$  values measured at the site.

In S4 well, located downstream of S1 (Fig. 1), samples from the deepest part showed much lower CMs concentrations than those from the upper part (Fig. 2), as observed also for chlorinated ethenes (Table A3). The CT and CF molar fractions were quite similar in Mar-10 and Mar-13 whereas the fraction of CF increased in Nov-14 at the upper part while total CMs concentration decreased (Fig. 2). However,  $\delta^{13}\text{C}_{\text{CT}}$  and  $\delta^{37}\text{Cl}_{\text{CT}}$  of S4 did not significantly change compared to S1 during the monitored period (Fig. 3A), indicating that observed changes in

CT and CF molar fractions are not attributed to in situ CT degradation, but proved CT degradation in trenches (Torrentó et al., 2014). This result agrees with the low concentrations of DCM and  $\text{CS}_2$  in this well (Table A3).

In S4, the most enriched  $\delta^{13}\text{C}_{\text{CF}}$  ( $-32.9 \pm 0.4$ , 425 m.a.s.l., Mar-13) and the most depleted  $\delta^{13}\text{C}_{\text{CF}}$  ( $-40.8 \pm 0.1\%$ , 419 m.a.s.l., Mar-13) values were 4‰ higher and 3‰ lower than  $\delta^{13}\text{C}_{\text{CF}}$  in the pit source, respectively (Table 1). Since CT isotopic composition remained quite stable for all depths during the studied period, these depleted  $\delta^{13}\text{C}_{\text{CF}}$  values cannot be linked to CT degradation.  $\delta^{13}\text{C}_{\text{CF}}$  enrichment might suggest CF degradation or influx of already isotope fractionated CF at the upper parts of S4 where the redox state was governed by the nitrate/nitrite equilibrium in aqueous solution (N system, in Fig. 1).

In S4, total CMs concentration and CT proportion are higher than in S1 (Figs. 1, 2 and Table A3) pointing out the detachment of the plume from S1 towards S4 through the fracture network. This is also supported by more depleted  $\delta^{13}\text{C}_{\text{CF}}$  values in S4 than in S1. In addition, in the latter available campaign,  $\delta^{37}\text{Cl}_{\text{CT}}$  values in S4 were more depleted than in S1 (Fig. 3A,B). These data suggest a lower extent of degradation for both compounds downstream. CMs moving downstream in the pit source's influence area might inhibit chlorinated ethenes biodegradation (Bagley et al., 2000), explaining the results previously reported by Palau et al. (2014).

### 3.2.2. Tank source's influence area

One of the most polluted wells at the site, S3, is located in the former tank where wastewater was spilled (Fig. 1). CMs concentration clearly decreased over time in the upper part of the well, while fluctuated without a clear trend at the middle and deepest points. A maximum CMs concentration (close to  $350 \mu\text{M}$ ) was reached at the deepest part in Nov-10 (Fig. 2). CF was the most abundant CM in all the studied campaigns, especially at the deepest parts, where it was almost an order of magnitude higher than CT (Fig. 2). High DCM contents were observed along all S3 levels, especially at the deepest part (up to  $102 \mu\text{M}$  in

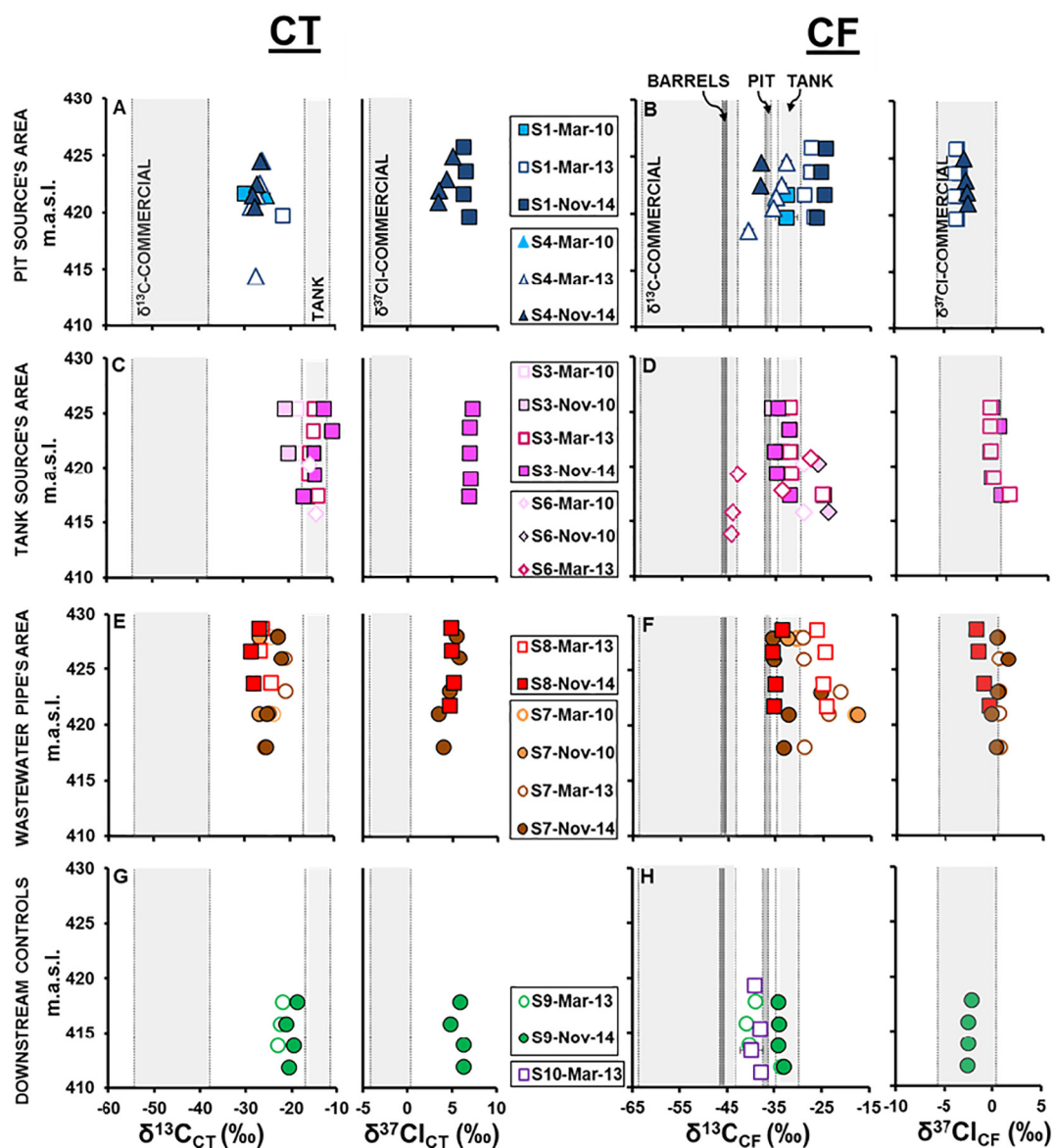


**Fig. 3.** Carbon and chlorine isotopic composition of CT (left panels) and CF (right panels) for wells S1 and S4 (A, B), S3 and S6 (C, D), S7 and S8 (E, F), and S9 and S10 (G, H) at different depths (m.a.s.l.) and campaigns. The shaded areas show the  $\delta^{13}\text{C}_{\text{CT}}$  and  $\delta^{13}\text{C}_{\text{CF}}$  range of commercial solvents, barrels, tank and pit sources, when available. In most cases, error bars are smaller than the symbols.

Mar-13, the 41% of the CMs molar fraction) (Fig. 2). In addition,  $\text{CS}_2$  values up to  $0.8 \mu\text{M}$  were found (Table A3).

$\delta^{13}\text{C}_{\text{CT}}$  values were very far from the isotopic composition range of commercial CT and fluctuated around the tank source range with offsets of up to  $+6.0\%$  and  $-5.0\%$  (Fig. 3C).  $\delta^{13}\text{C}_{\text{CT}}$  and  $\delta^{37}\text{Cl}_{\text{CT}}$  values (up to  $-10.3 \pm 0.3\%$  and  $+7.3 \pm 0.3\%$  (Fig. 3C), respectively) were the most enriched values of all wells and campaigns.  $\delta^{13}\text{C}_{\text{CT}}$  enriched in S3 over time, as well as from top to bottom in Mar-10 and Nov-10 (maximum difference of  $+5.2\%$ ). However, the opposite trend was observed in Nov-14, with up to a  $+6.5\%$  difference (Fig. 3C). This opposite trend could be due to the occurrence in parallel of different processes: 1) CT degradation inducing isotopic enrichment in  $^{13}\text{C}$ , more evident in the deepest parts and supported by a steady Eh controlled by Fe-system; and 2) new CT incoming depleting  $\delta^{13}\text{C}_{\text{CT}}$  values in the upper parts, especially in the early campaigns.

$\delta^{13}\text{C}_{\text{CF}}$  fluctuated over time within the limits of the tank and pit sources ranges (Fig. 3D), except at the deepest part, where  $\delta^{13}\text{C}_{\text{CF}}$  values were 5‰ more enriched than the rest of the well (Fig. 3D). As the same isotope pattern was observed for  $\delta^{37}\text{Cl}_{\text{CF}}$  values in Mar-13 and Nov-14 (enrichment of up to 1.9‰, Fig. 3D), CF degradation processes in the

deepest part of the well can be assumed. At shallower depths,  $\delta^{13}\text{C}_{\text{CF}}$  probably reflects a mixture of isotope effects associated with CF degradation and the continuous input of CF, as by-product of proved CT degradation and/or as incoming pollution.

In S3, only  $\delta^{13}\text{C}_{\text{DCM}}$  values from the deepest levels of Mar-13 and Nov-14 campaigns were available (from  $-41 \pm 1$  to  $-36 \pm 1\%$ , Table A3). They were in a range similar to that of the barrels and tank sources (from  $-42.1 \pm 0.5$  to  $-36 \pm 3\%$ , respectively) (Table 1). Nevertheless, this similar isotope range may have resulted from DCM coming from CF degradation. Thus, although high DCM concentrations at deep levels of S3 were detected comparing with the other wells (Fig. 2),  $\delta^{13}\text{C}_{\text{DCM}}$  shifts did not support unequivocal evidences of DCM origin or fate during the studied period.

In well S6, situated downstream from the tank source, total CMs concentration was much lower than in S3 for all campaigns (Fig. 2) and decreased over time. CF was the most abundant compound (up to  $51 \mu\text{M}$ ), with a concentration frequently an order of magnitude higher than CT. DCM and  $\text{CS}_2$  reached concentrations of  $0.7 \mu\text{M}$  and  $0.02 \mu\text{M}$ , respectively (Table A3). Due to the low CT concentration,  $\delta^{13}\text{C}_{\text{CT}}$  was measured in few samples and no data for  $\delta^{37}\text{Cl}_{\text{CT}}$  was obtained (Fig. 3C).

Determined  $\delta^{13}\text{C}_{\text{CT}}$  values ( $-15.2 \pm 0.5\%$  and  $-13.8 \pm 0.4\%$ ) are within the S3 and tank source values range. This fact hindered the identification of i) CT degradation and ii) whether the observed isotope ratios were the result of enriched CT transported from the former tank or latter degradation in S3 or S6. For CF in S6,  $\delta^{13}\text{C}_{\text{CF}}$  values in Mar-10 were 16‰ more enriched than latter in Mar-13 when the most negative values for all sampling wells and campaigns ( $-44.6 \pm 0.5\%$  Fig. 3D) were found. This latter value was within the range of the barrels and commercial CF (Fig. 3D) but it could also represent a CF by-product from a completely degraded CT with an isotopic signature similar to CT from commercial brands and barrels. Moreover, in Mar-13,  $\delta^{13}\text{C}_{\text{CF}}$  values increased from this depleted value at the bottom to a value similar to those found in previous campaigns at the top (Fig. 3D). Since new entrances of non-degraded CF from upstream areas seem improbable (attending to the enriched  $\delta^{13}\text{C}_{\text{CF}}$  values of S3 well over time, Fig. 3D), this behaviour might be explained by extensive CT degradation in S3-S6 area. Although the decrease in concentration and the Eh value controlled by Fe and N systems (Fig. 1) would support this hypothesis, it cannot be confirmed by  $\delta^{37}\text{Cl}_{\text{CF}}$  or any CT isotope data.

### 3.2.3. Wastewater pipe area

The S8 well, located upstream of the tank source at the point where the wastewater pipe was connected to the chemical plant (Fig. 1), showed low CMs concentrations with a maximum of 8  $\mu\text{M}$  at 427 m.a.s.l. in Mar-13 (Fig. 2). In general, CF was more abundant than CT. CMs concentration did not clearly decrease during the monitored period (Fig. 2), although in Nov-10 and Mar-13, CT and CF concentrations fell with depth down three orders of magnitude (Table A3). DCM and  $\text{CS}_2$  were present also in low concentrations (up to 0.1  $\mu\text{M}$  and 0.04  $\mu\text{M}$ , respectively).  $\delta^{13}\text{C}_{\text{CT}}$  values were depleted with respect to the tank source values ( $>10\%$ ), enriched compared to the range for commercial CT and values of Nov-14 (Fig. 3E) were similar to those found in S4 (Mar-13 and Nov-14) or in S1 (Mar-10, Fig. 3A). As a maximum  $\delta^{13}\text{C}_{\text{CT}}$  decrease of 4‰ was measured at the upper part (424 m.a.s.l.) between Mar-13 and Nov-14 (Fig. 3E), leaching processes could be suggested.  $\delta^{37}\text{Cl}_{\text{CT}}$  values (Nov-14) did not show a relevant enrichment in depth (Fig. 3E). For CF,  $\delta^{13}\text{C}_{\text{CF}}$  underwent more than a 10‰ decrease from Mar-13 to Nov-14 (Fig. 3F). The depleted  $\delta^{13}\text{C}_{\text{CF}}$  values of Nov-14 were close to the pit and tank values, but enriched with respect to the range determined for the barrels and commercial CF (Fig. 3F).

For the S7 well, CMs concentration in the upper part of S7 was always much higher than those of its deepest part and those of the rest of the wells (Fig. 2). Moreover, at 428 m.a.s.l., CMs concentration increased up to 632  $\mu\text{M}$  in Nov-14 (Fig. 2), consistently with the increase revealed in Nov-10. CT and CF molar ratios presented similar values at the upper part of S7, except in Mar-2013 when the molar ratio of DCM became significant and a decrease in total CMs concentration was observed. At depth, DCM and CF molar fractions decreased over time (Fig. 2).  $\text{CS}_2$  concentration values were only analysed for Mar-13 (up to 0.04  $\mu\text{M}$ ), preventing us to define if  $\text{CS}_2$  was yielded as a by-product.

Determined  $\delta^{13}\text{C}_{\text{CT}}$  values were between those from the tank source and those for commercial CT (Fig. 3E). The values fluctuated over campaigns with an enrichment of around 5‰ from the bottom to the top during Mar-13 and Nov-14 (Fig. 3E). This, together with a 2‰ enrichment of  $\delta^{37}\text{Cl}_{\text{CT}}$  values (Fig. 3E), may suggest reliable CT degradation at the upper part during the studied period.  $\delta^{13}\text{C}_{\text{CF}}$  also fluctuated over time and showed the most depleted values in Nov-14 (Fig. 3F). In contrast to CT, the strongest enrichment in  $^{13}\text{C}_{\text{CF}}$  was observed at the middle part (around 420 m.a.s.l.).  $\delta^{13}\text{C}_{\text{CF}}$  and  $\delta^{37}\text{Cl}_{\text{CF}}$  values measured in 2010 ( $-17.9 \pm 0.7$  and  $+1.6 \pm 0.5\%$ , respectively) (Fig. 3F, Table A5) were the most enriched values in all campaigns and wells. Therefore, despite the contribution of active leaching arriving from the unsaturated zone through the fracture network, the meaningful isotopic enrichment at the middle part, the high DCM molar fractions and the

decrease of Eh values with depth (Fig. 1, Fig. A1) evidenced the occurrence of CMs natural attenuation processes in this area.

### 3.2.4. Downstream controls

The S9 well, the furthest well downstream from the chemical plant and the highly affected area (Fig. 1), serves as outer control to establish if authorities should implement additional remediation measures. CMs concentrations were low (up to 10  $\mu\text{M}$ , Fig. 2) and CF was always more abundant than CT. In Nov-14, both CF, CT and DCM concentrations (up to 4, 0.9 and 0.8  $\mu\text{M}$ , respectively) (Table A3), exceeded the European Union (EU, 2008/105/CE) limits of 0.08, 0.02 and 0.2  $\mu\text{M}$ , respectively.  $\text{CS}_2$  concentrations were low (e.g. 0.04  $\mu\text{M}$  in Nov-14); nevertheless this compound is not regulated. The most negative  $\delta^{13}\text{C}_{\text{CT}}$  value in S9 ( $-22.97 \pm 0.02$ , Mar-13, Fig. 3G) was 7‰ more depleted than the most negative value of the tank source (Table 1), but was very enriched compared to the range obtained for commercial CT. CMs degradation processes would have affected the tank only after certain original CMs pollution had already reached the saturated zone downstream, explaining the high CT fractionation detected in 2003 and 2004 source's sampling in comparison to some depleted CT values in wells.

In S10 well, located downstream of S6, at the other side of the creek (Fig. 1), the highest concentration of CMs was found in Mar-13, with up to 0.1  $\mu\text{M}$  CT and 0.3  $\mu\text{M}$  CF, both slightly above the EU limits. Measured  $\text{CS}_2$  contents were low ( $\leq 0.01$   $\mu\text{M}$ ). Thus, pollution has not strongly affected the groundwater eastbound moving far beyond this well. Low concentration of CMs only allowed for  $\delta^{13}\text{C}_{\text{CF}}$  values in Mar-13 (Fig. 3H).

### 3.3. Degradation pathways study

This subsection evaluates the potential of 2D-CSIA approach to identify CMs degradation pathways in complex fractured aquifer. To this end, dual C-Cl isotope plots of the different multilevel wells were compared with literature data. Fig. 4 shows the  $\delta^{13}\text{C}$  vs.  $\delta^{37}\text{Cl}$  data of CT and CF obtained in Mar-13 and Nov-14 campaigns and establishes the origin of C-Cl  $\Lambda$  values. All these data are plotted together with values from sources prior to their removal and from commercial solvents. Moreover, statistical comparison of the obtained C-Cl  $\Lambda$  values from wells with those of different degradation mechanisms or pathways already reported in literature is also included in this section.

The CT dual C-Cl isotope plot (Fig. 4) supports that CT in S4 and S8 wells, despite the distance between the wells (Fig. 1), likely comes from the same spilled CT. Similar CMs carbon isotopic mass balance values ( $\delta^{13}\text{C}_{\text{SUM}}$ , see Eq. (A1)) for the tank, before its removal, and for S3 and S7 over time, especially in the shallowest parts, also point out to a single mixture of original spilled CMs in all over Òdena site (Fig. A2). CT in S8 and S4 showed negligible  $\delta^{13}\text{C}$  variation but certain  $\delta^{37}\text{Cl}$  enrichment (Fig. 4). This enrichment might be attributable to Cl isotope fractionation processes in the unsaturated zone inasmuch as normal isotope effects of both reactive and non-reactive processes (such as diffusion-controlled vaporization) in the unsaturated zone accumulate for Cl (Jeannotat and Hunkeler, 2012). Since there are not available barrel values (Table 1), the most depleted S4 values ( $+3.5\%$  for  $\delta^{37}\text{Cl}$  and  $-28.2\%$  for  $\delta^{13}\text{C}$ ) was considered as origin for slope calculations.

CT samples in Fig. 4 showed a general C and Cl enrichment trend confirming CT degradation processes. If S3, S7 and S9 values are considered together with the above-mentioned origin, the obtained  $\Lambda$  value ( $4 \pm 1$ ,  $R^2 = 0.82$ ) is statistically similar (ANCOVA  $p > 0.05$ ) to that found in laboratory experiments for CT hydrogenolysis combined with CT thiolytic reduction (Py in Fig. 4, Rodríguez-Fernández et al., 2018b). Despite this general observation, a separate study of each well is provided since it is interesting to discern different contributions of these pathways under each wells' conditions.

In this sense, CT samples of S3 show a  $\Lambda$  value ( $4 \pm 2$ ,  $R^2 = 0.91$ ) statistically similar to the reference slope for net hydrogenolysis (Fe

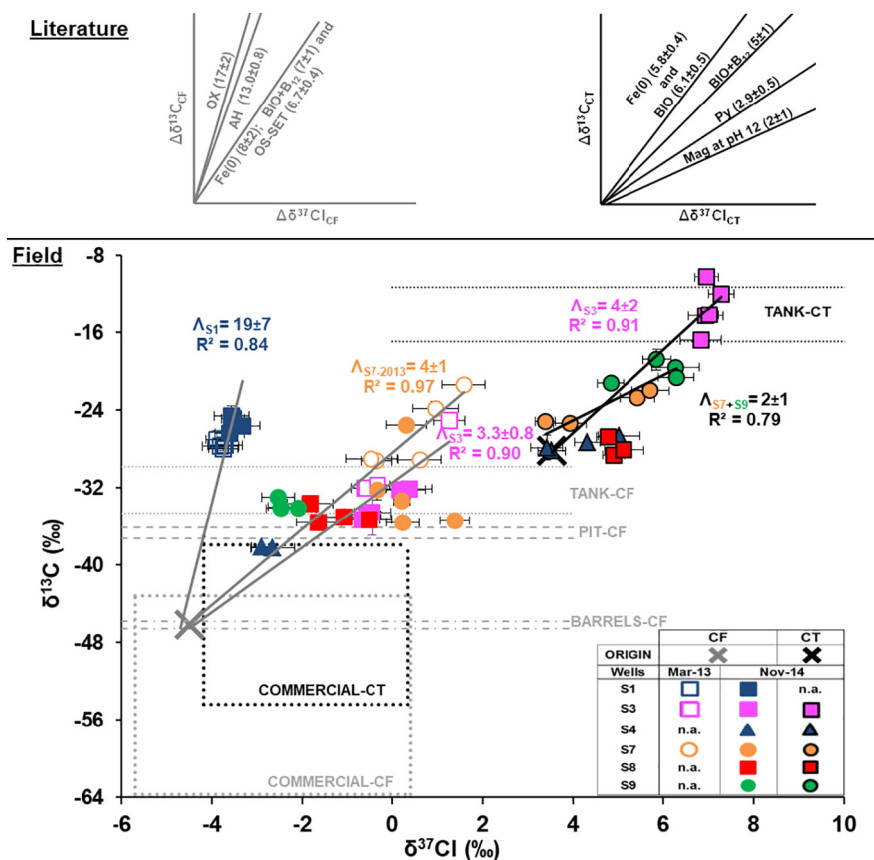


**Fig. 4.** Dual C-Cl isotope plot for CT and CF data from sampling wells (S-number) in Mar-13 and Nov-14 campaigns (n.a. = data not available). Error bars show uncertainty in  $\delta^{13}\text{C}$  and  $\delta^{37}\text{Cl}$  values.  $\delta^{13}\text{C}$  of the sources (barrels, pit and tank) sampled prior to their removal and  $\delta^{13}\text{C}$  and  $\delta^{37}\text{Cl}$  of commercial compounds are represented in black and grey dashed lines and boxes for CT and CF, respectively. Upper plots show: CF (left) reference slopes of oxidation (OX), alkaline hydrolysis (AH) and hydrogenolysis + reductive elimination (Fe(0)) from [Torrentó et al. \(2017\)](#); outer-sphere single electron transfer (OS-SET) from [Heckel et al. \(2017a\)](#); and CF inferred pathways from biodegradation with vitamin B<sub>12</sub> (BIO + B<sub>12</sub>) (Rodríguez-Fernández et al., 2018a); as well as CT (right) reference slopes of hydrogenolysis (Fe(0), Rodríguez-Fernández et al., 2018b) and inferred pathways from biodegradation with vitamin B<sub>12</sub> from microcosms (BIO and + B<sub>12</sub>, Rodríguez-Fernández et al., 2018a) and from degradation by pyrite (Py) and by magnetite (Mag) at pH 12, (Rodríguez-Fernández et al., 2018b). The CT and CF slopes ( $\Lambda_{\text{well}}$ ) are shown relative to the most depleted isotope values detected in the field (referred as 'Origin' in legend).

(0) reaction in Fig. 4,  $\Lambda = 5.8 \pm 0.4$ , Rodríguez-Fernández et al., 2018b). The obtained  $\Lambda$  value for S3 is also consistent i) with an OS-SET mechanism (Heckel et al., 2017a) ( $6.7 \pm 0.4$ ); ii) with biodegradation obtained in microcosms experiments using sediment slurry from this well ( $6.1 \pm 0.5$ , Rodríguez-Fernández et al., 2018a), and iii) with a reductive pathway involving *Pseudomonas stutzeri*, obtained when vitamin B<sub>12</sub> was added in the slurry ( $5 \pm 1$ , Rodríguez-Fernández et al., 2018a). This result confirmed in situ CT anaerobic reduction in S3, consistently with the steady Eh controlled by the Fe-system during the studied period (Fig. A1). Nevertheless, due to the relatively high CS<sub>2</sub> amount detected in S3 a certain contribution of thiolitic CT reduction mediated by iron sulfides like pyrite (Davis et al., 2003; Rodríguez-Fernández et al., 2018b) or biotically-mediated by sulfate-reducing bacteria (Koenig et al., 2012) cannot be excluded. This hypothesis is supported by the decrease in total dissolved iron and sulfate concentrations and by a  $\delta^{34}\text{S}$  enrichment in  $\text{SO}_4^{2-}$  (from  $+14 \pm 0.2$  to  $+22 \pm 0.2\text{‰}$ ) with depth in S3 (Table A1). Therefore, although the dual slope revealed hydrogenolysis as the main pathway, little involvement of thiolitic or hydrolytic reduction might be possible (Py and Mag reactions, respectively in Fig. 4, Rodríguez-Fernández et al., 2018b).

Assuming reductive biodegradation as the main CT degradation process, the maximum extent D (% Eq. (1)) in S3 would be  $72 \pm 11\%$ , which is estimated using  $\epsilon_{\text{CT}}$  from S3 microcosm experiments ( $-16 \pm 6\text{‰}$ ) (Rodríguez-Fernández et al., 2018a), the most positive value for CT in S3 as  $\delta^{13}\text{C}_{\text{CT}}$  ( $-10.3 \pm 0.3\text{‰}$ ), and the most depleted value found in the field as  $\delta^{13}\text{C}_0$  ( $-30.0 \pm 0.5\text{‰}$ ). This D value in S3 is probably a conservative estimate since leaching of less-degraded CT from the unsaturated

zone could mask  $\delta^{13}\text{C}$  values (see further discussion in Isotopic mass balance section in SI).

Since S7 and S9 showed similar slopes, isotope data of CT from these wells were combined. The resulting  $\Lambda$  ( $2 \pm 1$ ,  $R^2 = 0.79$ ) is statistically similar to that inferred with Py, suggesting that both CT hydrogenolysis with CT thiolitic reduction might occur (Py in Fig. 4, Rodríguez-Fernández et al., 2018b). However, the contribution of CT thiolitic reduction is revealed higher in S7 and S9 than in S3, attending to 2D-CSIA approach and as it was also confirmed by  $\delta^{13}\text{C}_{\text{SUM}}$  comparison between S3 and S7 in Nov-10 (see SI). CT reduction pathways are consistent with the low Eh values measured in the deepest parts of S7 (Fig. A1). The maximum D of CT would be  $84 \pm 6\%$  for S7 and  $90 \pm 4\%$  for S9 assuming a combination of hydrogenolysis and thiolitic reduction pathways (Fig. 4) and using a  $\epsilon_{\text{CT}} = -5 \pm 2\text{‰}$ , (Py, Rodríguez-Fernández et al., 2018b), the most enriched values for CT in S7 and S9 as  $\delta^{13}\text{C}_{\text{CT}}$  ( $-21.0 \pm 0.3\text{‰}$  and  $-19 \pm 1\text{‰}$ , respectively), and the most depleted value found in the field as  $\delta^{13}\text{C}_0$  ( $-30.0 \pm 0.5\text{‰}$ ).

The interpretation of the determined dual C-Cl isotope trends for CF (Fig. 4) should consider that CF can also be produced by CT degradation besides being degraded, similarly to trichloroethene or cis-1,2-dichloroethene in previous studies (Badin et al., 2016). Thus, comparison with reported  $\Lambda$  values from literature is not straightforward. According to Hunkeler et al. (2009), in a reaction where CF is a by-product,  $\delta^{37}\text{Cl}_{\text{CF}}$  cannot be more depleted than the initial  $\delta^{37}\text{Cl}$  value of the parent compound CT (assuming no secondary isotopic effects). In Òdena, all field  $\delta^{37}\text{Cl}_{\text{CF}}$  values plotted in Fig. 4 are more depleted than  $\delta^{37}\text{Cl}_{\text{CT}}$  ones, confirming the predominance of CF as a parent compound.



Moreover, CF was present in the sources as a pure phase in the barrels (Table 1) and represented >70% of the molar fraction among CMs in the other sources. These two arguments support a predominance of CF as a parent compound and suggest that, although some contribution of CF as by-product is undeniable, the obtained CF  $\Lambda$  values are primarily controlled by CF degradation.

Values for pit source's influence area (S1 and S4), clearly plot in a different pattern than those from the rest of the wells (Fig. 4). As it was argued previously for CT, a single original CMs mixture is considered and reactive processes that fractionate inversely are discarded for the interpretation of the data since they have not been described yet. Shifts towards heavier  $\delta^{37}\text{Cl}$  over time due to source aging are also expected for CF. The most depleted  $\delta^{37}\text{Cl}_{\text{CF}}$  value determined in the field site was  $-3.9 \pm 0.6\%$ , which was measured in S1 (422 m.a.s.l., Mar-13), consistent with the most depleted  $\delta^{37}\text{Cl}_{\text{CF}}$  commercial values. Since calculations for estimating the  $\delta^{37}\text{Cl}_0$  of CF require the unavailable  $\epsilon\text{Cl}$  of CF diffusion in Òdena's soil, the SD of the most depleted  $\delta^{37}\text{Cl}_{\text{CF}}$  value was considered for obtaining the value used as origin for slope calculations, i.e.  $\delta^{37}\text{Cl}_{\text{CF}} = -4.5\%$ . In the case of C, the most depleted  $\delta^{13}\text{C}_{\text{CF}}$  determined in the field site (barrels,  $-46.2 \pm 0.4\%$ , in the upper range of for commercial CF) was considered as the outset for the slope (Table 1, Fig. 4).

S1 data from Mar-13 and Nov-14 campaigns form a cluster while data of the other wells distribute along a clear trend (Fig. 4). This different behaviour could be related to the absence of CMs leaching in S1, while in the other wells, leaching was proved. The obtained slope for S1 ( $\Lambda = 19 \pm 7$ ,  $R^2 = 0.84$ ) was consistent with CF oxidation (OX, Fig. 4) or with CF alkaline hydrolysis (AH, Fig. 4) (ANCOVA,  $p > 0.05$ ) (Torrentó et al., 2017). CF oxidation in the pit source's influence area might be supported by an Eh evolution from Fe-controlled conditions in 2006 and 2007 towards more oxidising conditions in the latter campaigns (Fig. 1, Fig. A1) which is consistent with open air spills in the pit source during chemical plant activity (Palau et al., 2014). Aerobic CF cometabolism is supported by the presence of BTEXs in the studied field site. BTEXs can act as a primary substrate (carbon source) of monooxygenases (Cappelletti et al., 2012) and they were found ranging from 4 to 4000  $\mu\text{g/L}$  in wells located in the source's areas in Mar-13. Alkaline hydrolysis might also be plausible given the hydraulic conductivity between the trench, where CF alkaline hydrolysis takes place, and the S1 well (Torrentó et al., 2014). Complementary tools would be necessary to distinguish both processes.

The CF dual C-Cl isotope slopes are only linear considering S3 and S7 wells, thus, wells S4, S8 and S9 were not included in  $\Lambda$  calculations. The dual C-Cl isotope slopes observed for CF in S3 (Mar-13 and Nov-14) and S7 (Mar-13) are  $\Lambda = 3.3 \pm 0.8$  ( $R^2 = 0.90$ ) and  $4 \pm 1$  ( $R^2 = 0.97$ ), respectively, considering the same CF origin as for S1 well. Both  $\Lambda$  values are more similar to CF reduction processes (Fe(0) and BIO + B12, Fig. 4, Rodríguez-Fernández et al., 2018a, 2018b) than to CF oxidation or alkaline hydrolysis (OX and AH, Fig. 4, Torrentó et al., 2017), in accordance with the redox conditions (Fig. 1) and with the presence of DCM indicative of hydrogenolysis (Fig. 2). The lack of statistical coincidence between CF  $\Lambda$  values of wells S3 and S7 and the available reference values for reduction processes could be attributed to 1) mixing of degraded CF with pollutant continuously being leached into the saturated zone that in turn, might be continuously affected by isotope fractionation processes; 2) chlorine isotope fractionation by a non-reactive processes, such as diffusion (Jeannotat and Hunkeler, 2012) that might explain lower S3 and S7 CF slopes regarding the reference slopes; 3) certain influence of CF as by-product and/or 4) the existence of other non-characterized CF degradation pathways.

#### 4. Conclusions

Although Òdena is a complex polluted site, it has been shown that the identification of CMs degradation by-products and the long-term monitoring of CMs concentration and of  $\delta^{13}\text{C}$  and redox shifts are

valuable tools for disclosing the effects in CMs of the removal of the pollutant sources and for detecting CMs natural attenuation. Moreover, CSIA and CMs concentration monitoring have been useful tools to identify the aging of the pollution sources and the existence of still active leaching source zones.

Almost all samples from wells and sources (before the removal, 2002–2005) were enriched in  $^{13}\text{C}$  with respect to CT and CF commercial values. Unexpectedly,  $\delta^{13}\text{C}$  values of CT from tank source were more enriched than those of all groundwater samples (except for the highly degraded CT in S3 well). Both observations revealed i) the occurrence of strong isotope fractionation processes during industrial activities or during sources aging in the unsaturated zone before source's removal, and ii) an important leaching to the saturated zone previous to the CMs isotope fractionation in sources. Thus, the most depleted isotope CMs values found in the Òdena site (S1 and S4 wells) and the  $\delta^{13}\text{C}_{\text{CF}}$  value from barrels in 2002 were considered as representative of the CT and CF isotopic composition of the original source. Therefore, results indicate that values found in aged sources should be treated with caution, when evaluating and quantifying current field degradation.

The monitoring methodologies also evidenced that in the pit source's influence area, the focus of CMs pollution was detached from S1 and moved downwards to S4 well, confirming that the source removal was effective and that no new CMs entered in this part of the plume. Nevertheless, they also revealed that the removal of the tank and wastewater pipe sources was incomplete because new CMs incomings were still arriving at S3, S7 and S8 wells during the monitoring time and the plume seemed still active. The S7 well was of special concern because leaching of CMs prevailed, and caused the highest CMs concentrations in the field site during the studied period. The furthest well downstream from the chemical plant (S9) showed CMs concentration values that exceeded the legal threshold values. Despite this fact, important CT and CF isotope fractionation processes have been identified in the wells located close to the former disposal areas (S1, S3 and S7), proving that CT and CF natural attenuation processes exist.

The use of dual element CSIA allowed the identification of the degradation pathways occurring at different areas of this fractured aquifer. CT reductive pathways were confirmed in S3, S7 and S9 wells, where CT degradation extents over 90% were estimated. Results suggest that CF oxidative degradation might have occurred at the former pit source area (S1 well), in consistency with open air spills documented in this area and with the observed evolution of porewater redox conditions towards more oxidising values after source removal. However, dual isotope slope in this area also fitted with CF alkaline hydrolysis occurring in groundwater coming from the upstream remediation trench (Torrentó et al., 2014), and therefore, complementary tools are needed for distinguishing both processes. For instance, hydrogen isotopes analysis (i.e.,  $\delta^2\text{H}$ ), or active microbial population assessment (e.g. monooxygenase-encoding genes or species) would be useful for distinguishing between both pathways. Finally, results suggest that in S3 and S7 wells, CF degradation is due to reductive processes.

This research shows for the first time that 2D-CSIA is a valuable tool for satisfactorily detecting and identifying CMs natural attenuation processes in fractured aquifers. Therefore, it is a promising approach to assess tailored remediation strategies in complex polluted field sites and for further monitoring them over time.

#### Acknowledgements

This research was supported by a Marie Curie Career Integration Grant in the framework of IMOTEC-BOX project (PCIG9-GA-2011-293808), the Spanish Government REMEDIATION (CGL2014-57215-C4-1-R AEI/FEDER, EU) and PACE-ISOTEC (CGL2017-87216-C4-1-R AEI/FEDER, EU) projects, and the Catalan Government project 2017SGR-1733. We thank the Agència Catalana de l'Aigua (ACA) for their support, the Agència de Residus de Catalunya (ARC) for allowing us to work in the monitored Òdena site, the CCIT-UB for the technical

assistance, and C. Audí-Miró, A. Follia, A. Grau, M. Moreno, M. de Olamendi and X. Wei for their support in field campaigns. D. Rodríguez-Fernández and M. Rosell acknowledge FPU2012/01615 and Ramón y Cajal contract (RYC-2012-11920), respectively. We thank the editor and the anonymous reviewers for their comments.

## Appendix A. Supplementary data

Supplementary data to this article can be found online at <https://doi.org/10.1016/j.scitotenv.2018.07.130>.

## References

- Audí-Miró, C., Cretnik, S., Torrentó, C., Rosell, M., Shouakar-Stash, O., Otero, N., Palau, J., Elsner, M., Soler, A., 2015. C, Cl and H compound-specific isotope analysis to assess natural versus Fe(0) barrier-induced degradation of chlorinated ethenes at a contaminated site. *J. Hazard. Mater.* 299:747–754. <https://doi.org/10.1016/j.jhazmat.2015.06.052>.
- Badin, A., Buttet, G., Maillard, J., Holliger, C., Hunkeler, D., 2014. Multiple dual C-Cl isotope patterns associated with reductive dechlorination of tetrachloroethene. *Environ. Sci. Technol.* 48:9179–9186. <https://doi.org/10.1021/es500822d>.
- Badin, A., Broholm, M.M., Jacobsen, C.S., Palau, J., Dennis, P., Hunkeler, D., 2016. Identification of abiotic and biotic reductive dechlorination in a chlorinated ethene plume after thermal source remediation by means of isotopic and molecular biology tools. *J. Contam. Hydrol.* <https://doi.org/10.1016/j.jconhyd.2016.05.003>.
- Baertschi, P., Kuhn, W., Kuhn, H., 1953. Fractionation of isotopes by distillation of some organic substances. *Nature* 171, 1018–1020.
- Bagley, D.M., Lalonde, M., Kaserov, V., Stasiuk, K.E., Sleep, B.E., 2000. Acclimation of anaerobic systems to biodegrade tetrachloroethene in the presence of carbon tetrachloride and chloroform. *Water Res.* 34:171–178. [https://doi.org/10.1016/S0043-1354\(99\)00121-9](https://doi.org/10.1016/S0043-1354(99)00121-9).
- Bernstein, A., Shouakar-stash, O., Ebert, K., Laskov, C., Hunkeler, D., Jeannotat, S., Sakaguchi-Söder, K., Laaks, J., Jochmann, M.A., Cretnik, S., Jager, J., Haderlein, S.B., Schmidt, T.C., Aravena, R., Elsner, M., 2011. Compound-specific chlorine isotope analysis: a comparison of gas chromatography/isotope ratio mass spectrometry and gas chromatography/quadrupole mass spectrometry methods in an interlaboratory study. *Anal. Chem.* 83:7624–7634. <https://doi.org/10.1021/ac200516c>.
- Cappelletti, M., Frascari, D., Zannoni, D., Fedi, S., 2012. Microbial degradation of chloroform. *Appl. Microbiol. Biotechnol.* 96:1395–1409. <https://doi.org/10.1007/s00253-012-4494-1>.
- Chan, C.C.H., Mundle, S.O.C., Eckert, T., Liang, X., Tang, S., Lacrampe-Couloume, G., Edwards, E.A., Sherwood Lollar, B., 2012. Large carbon isotope fractionation during biodegradation of chloroform by *Dehalobacter* cultures. *Environ. Sci. Technol.* 46:10154–10160. <https://doi.org/10.1021/es3010317>.
- Coplen, 2011. Guidelines and recommended terms for expression of stable-isotope-ratio and gas-ratio measurement results. *Rapid Commun. Mass Spectrom.* 2011 (25), 2538–2560.
- Davis, A., Fennemore, G.G., Peck, C., Walker, C.R., McLwraith, J., Thomas, S., 2003. Degradation of carbon tetrachloride in a reducing groundwater environment: implications for natural attenuation. *Appl. Geochem.* 18:503–525. [https://doi.org/10.1016/S0883-2927\(02\)00102-6](https://doi.org/10.1016/S0883-2927(02)00102-6).
- Deshpande, N.P., Wong, Y.K., Manfield, M., Wilkins, M.R., Lee, M., 2013. Genome sequence of *Dehalobacter* UNSVDHB, a chloroform-dechlorinating bacterium. *Genome Announc.* 1:1–2. <https://doi.org/10.1186/1471-2105-11-4857>.
- Devlin, J.F., Muller, D., 1999. Field and laboratory studies of carbon tetrachloride transformation in a sandy aquifer under sulfate reducing conditions. *Environ. Sci. Technol.* 33:1021–1027. <https://doi.org/10.1021/es9806884>.
- Ding, C., Zhao, S., He, J., 2014. A *Desulfitobacterium* sp. strain PR reductively dechlorinates both 1,1,1-trichloroethane and chloroform. *Environ. Microbiol.* 16:3387–3397. <https://doi.org/10.1111/1462-2920.12387>.
- Dogramaci, S.S., Herczeg, A.L., Schiff, S.L., Bone, Y., 2001. Controls on  $\delta^{34}\text{S}$  and  $\delta^{18}\text{O}$  of dissolved sulfate in aquifers of the Murray Basin, Australia and their use as indicators of flow processes. *Appl. Geochem.* 16:475–488. [https://doi.org/10.1016/S0883-2927\(00\)00052-4](https://doi.org/10.1016/S0883-2927(00)00052-4).
- Duhamel, M., Wehr, S.D., Yu, L., Rizvi, H., Seepersad, D., Dworatzek, S., Cox, E.E., Edwards, E.A., 2002. Comparison of anaerobic dechlorinating enrichment cultures maintained on tetrachloroethene, trichloroethene, cis-dichloroethene and vinyl chloride. *Water Res.* 36:4193–4202. [https://doi.org/10.1016/S0043-1354\(02\)00151-3](https://doi.org/10.1016/S0043-1354(02)00151-3).
- European Environment Agency (EEA), 2014. Progress in management of contaminated sites (CSI 015) [WWW document]. <http://www.eea.europa.eu/data-and-maps/indicators/progress-in-management-of-contaminated-sites-3/assessment>, Accessed date: 18 April 2017.
- European Union, 2008. Directive 2008/105/CE Related to the Rules of Environmental Quality Within Water Policies. Official Journal of the European Union.
- Field, J.A., Sierra-Alvarez, R., 2004. Biodegradability of chlorinated solvents and related chlorinated aliphatic compounds. *Rev. Environ. Sci. Biotechnol.* 3:185–254. <https://doi.org/10.1007/s11157-004-4733-8>.
- Futagami, T., Yamaguchi, T., Nakayama, S.I., Goto, M., Furukawa, K., 2006. Effects of chloromethanes on growth and of deletion of the *pce* gene cluster in dehalorespiring *Desulfitobacterium hafniense* strain Y51. *Appl. Environ. Microbiol.* 72:5998–6003. <https://doi.org/10.1128/AEM.00979-06>.
- Futagami, T., Fukaki, Y., Fujihara, H., Takegawa, K., Goto, M., Furukawa, K., 2013. Evaluation of the inhibitory effects of chloroform on ortho-chlorophenol- and chloroethene-dechlorinating *Desulfitobacterium* strains. *AMB Express* 3:1–8. <https://doi.org/10.1186/2191-0855-3-30>.
- Grosterm, A., Duhamel, M., Dworatzek, S., Edwards, E.A., 2010. Chloroform respiration to dichloromethane by a *Dehalobacter* population. *Environ. Microbiol.* 12:1053–1060. <https://doi.org/10.1111/j.1462-2920.2009.02150.x>.
- He, Y.T., Wilson, J.T., Su, C., Wilkin, R.T., 2015. Review of abiotic degradation of chlorinated solvents by reactive iron minerals in aquifers. *Groundw. Monit. Remediat.* 35:57–75. <https://doi.org/10.1111/gwmmr.12111>.
- Heckel, B., Cretnik, S., Kliegman, S., Shouakar-Stash, O., McNeill, K., Elsner, M., 2017a. Reductive outer-sphere single electron transfer is an exception rather than the rule in natural and engineered chlorinated ethene dehalogenation. *Environ. Sci. Technol.* 51:9663–9673. <https://doi.org/10.1021/acs.est.7b01447>.
- Heckel, B., Rodríguez-Fernández, D., Torrentó, C., Meyer, A., Palau, J., Domènech, C., Rosell, M., Soler, A., Hunkeler, D., Elsner, M., 2017b. Compound-specific chlorine isotope analysis of tetrachloromethane and trichloromethane by gas chromatography-isotope ratio mass spectrometry vs gas chromatography-quadrupole mass spectrometry: method development and evaluation of precision and trueness. *Anal. Chem.* 89:3411–3420. <https://doi.org/10.1021/acs.analchem.6b04129>.
- Holt, B.D., Sturchio, N.C., Abrajano, T.A., Heraty, L.J., 1997. Conversion of chlorinated volatile organic compounds to carbon dioxide and methyl chloride for isotopic analysis of carbon and chlorine. *Anal. Chem.* 69:2727–2733. <https://doi.org/10.1021/ac961096b>.
- Hunkeler, D., Aravena, R., 2000. Determination of compound-specific carbon isotope ratios of chlorinated methanes, ethanes, and ethenes in aqueous samples. *Environ. Sci. Technol.* 34:2839–2844. <https://doi.org/10.1021/es991178s>.
- Hunkeler, D., Aravena, R., Berry-Spark, K., Cox, E., 2005. Assessment of degradation pathways in an aquifer with mixed chlorinated hydrocarbon contamination using stable isotope analysis. *Environ. Sci. Technol.* 39:5975–5981. <https://doi.org/10.1021/es048464a>.
- Hunkeler, D., Meckenstock, R.U., Lollar, B.S., Schmidt, T.C., Wilson, J.T., 2008. A Guide for Assessing Biodegradation and Source Identification of Organic Ground Water Contaminants Using Compound Specific Isotope Analysis (CSIA). EPA.
- Hunkeler, D., Van Breukelen, B.M., Elsner, M., 2009. Modeling chlorine isotope trends during sequential transformation of chlorinated ethenes. *Environ. Sci. Technol.* 43:6750–6756. <https://doi.org/10.1021/es900579z>.
- Imfeld, G., Nijenhuis, I., Nikolausz, M., Zeiger, S., Paschke, H., Drangmeister, J., Grossmann, J., Richnow, H.H., Weber, S., 2008. Assessment of in situ degradation of chlorinated ethenes and bacterial community structure in a complex contaminated groundwater system. *Water Res.* 42:871–882. <https://doi.org/10.1016/j.watres.2007.08.035>.
- Jeannotat, S., Hunkeler, D., 2012. Chlorine and carbon isotopes fractionation during volatilization and diffusive transport of trichloroethene in the unsaturated zone. *Environ. Sci. Technol.* 46:3169–3176. <https://doi.org/10.1021/es203547p>.
- Jeannotat, S., Hunkeler, D., 2013. Can soil gas VOCs be related to groundwater plumes based on their isotope signature? *Environ. Sci. Technol.* 47:12115–12122. <https://doi.org/10.1021/es4010703>.
- Jendrzewski, N., Eggenkamp, H.G.M., Coleman, M.L., 2001. Characterisation of chlorinated hydrocarbons from chlorine and carbon isotopic compositions: scope of application to environmental problems. *Appl. Geochem.* 16:1021–1031. [https://doi.org/10.1016/S0883-2927\(00\)00083-4](https://doi.org/10.1016/S0883-2927(00)00083-4).
- Justicia-Leon, S.D., Higgins, S., Mack, E.E., Griffiths, D.R., Tang, S., Edwards, E.A., Löffler, F.E., 2014. Bioaugmentation with distinct *Dehalobacter* strains achieves chloroform detoxification in microcosms. *Environ. Sci. Technol.* 48:1851–1858. <https://doi.org/10.1021/es403582f>.
- Kaown, D., Shouakar-Stash, O., Yang, J., Hyun, Y., Lee, K.K., 2014. Identification of multiple sources of groundwater contamination by dual isotopes. *Groundwater* 52:875–885. <https://doi.org/10.1111/gwat.12130>.
- Kirtland, B.C., Aelion, C.M., Stone, P.A., Hunkeler, D., 2003. Isotopic and geochemical assessment of in situ biodegradation of chlorinated hydrocarbons. *Environ. Sci. Technol.* 37:4205–4212. <https://doi.org/10.1021/es034046e>.
- Koenig, J.C., Lee, M.J., Manfield, M., 2012. Successful microcosm demonstration of a strategy for biodegradation of a mixture of carbon tetrachloride and perchloroethene harnessing sulfate reducing and dehalorespiring bacteria. *J. Hazard. Mater.* 219–220:169–175. <https://doi.org/10.1016/j.jhazmat.2012.03.076>.
- Kuder, T., Van Breukelen, B.M., Vanderford, M., Philp, P., 2013. 3D-CSIA: carbon, chlorine, and hydrogen isotope fractionation in transformation of TCE to ethene by a *Dehalococcoides* culture. *Environ. Sci. Technol.* 47:9668–9677. <https://doi.org/10.1021/es400463p>.
- Lee, M., Low, A., Zemb, O., Koenig, J., Michaelsen, A., Manfield, M., 2012. Complete chloroform dechlorination by organochlorine respiration and fermentation. *Environ. Microbiol.* 14:883–894. <https://doi.org/10.1111/j.1462-2920.2011.02656.x>.
- Lewis, T.A., Crawford, R.L., 1995. Transformation of carbon tetrachloride via sulfur and oxygen substitution by *Pseudomonas* sp. strain KC. *J. Bacteriol.* 177, 2204–2208.
- Lima, G. da P., Sleep, B.E., 2010. The impact of carbon tetrachloride on an anaerobic methanol-degrading microbial community. *Water Air Soil Pollut.* 212:357–368. <https://doi.org/10.1007/s11270-010-0350-z>.
- Martín-González, L., Mortan, S.H., Rosell, M., Parladé, E., Martínez-Alonso, M., Gaju, N., Caminal, G., Adrian, L., Marco-Urrea, E., 2015. Stable carbon isotope fractionation during 1,2-dichloropropane-to-propene transformation by an enrichment culture containing *Dehalogenimonas* strains and a *dcpA* gene. *Environ. Sci. Technol.* 49:8666–8674. <https://doi.org/10.1021/acs.est.5b00929>.
- Maymó-Gatell, X., Nijenhuis, I., Zinder, S.H., 2001. Reductive dechlorination of cis-1,2-dichloroethene and vinyl chloride by *Dehalococcoides ethenogenes*. *Environ. Sci. Technol.* 35:516–521. <https://doi.org/10.1021/es001285i>.
- Nijenhuis, I., Schmidt, M., Pellegatti, E., Paramatti, E., Richnow, H.H., Gargini, A., 2013. A stable isotope approach for source apportionment of chlorinated ethene plumes at

- a complex multi-contamination events urban site. *J. Contam. Hydrol.* 153:92–105. <https://doi.org/10.1016/j.jconhyd.2013.06.004>.
- Palau, J., Marchesi, M., Chambon, J.C.C., Aravena, R., Canals, À., Binning, P.J., Bjerg, P.L., Otero, N., Soler, A., 2014. Multi-isotope (carbon and chlorine) analysis for fingerprinting and site characterization at a fractured bedrock aquifer contaminated by chlorinated ethenes. *Sci. Total Environ.* 475:61–70. <https://doi.org/10.1016/j.scitotenv.2013.12.059>.
- Palau, J., Jamin, P., Badin, A., Vanhecke, N., Haerens, B., Brouyère, S., Hunkeler, D., 2016. Use of dual carbon-chlorine isotope analysis to assess the degradation pathways of 1,1,1-trichloroethane in groundwater. *Water Res.* 92:235–243. <https://doi.org/10.1016/j.watres.2016.01.057>.
- Penny, C., Vuilleumier, S., Bringel, F., 2010. Microbial degradation of tetrachloromethane: mechanisms and perspectives for bioremediation. *FEMS Microbiol. Ecol.* 74:257–275. <https://doi.org/10.1111/j.1574-6941.2010.00935.x>.
- Puig, R., Folch, A., Menció, A., Soler, A., Mas-Pla, J., 2013. Multi-isotopic study ( $^{15}\text{N}$ ,  $^{34}\text{S}$ ,  $^{18}\text{O}$ ,  $^{13}\text{C}$ ) to identify processes affecting nitrate and sulfate in response to local and regional groundwater mixing in a large-scale flow system. *Appl. Geochem.* 32: 129–141. <https://doi.org/10.1016/j.apgeochem.2012.10.014>.
- Puigdomènech, I., 2010. MEDUSA (Make Equilibrium Diagrams Using Sophisticated Algorithms) Windows Interface to the MS-DOS Versions of INPUT, SED and PREDOM (FORTRAN Programs Drawing Chemical Equilibrium Diagrams).
- Puigserver, D., Carmona, J.M., Cortés, A., Viladevall, M., Nieto, J.M., Grifoll, M., Vila, J., Parker, B.L., 2013. Subsoil heterogeneities controlling porewater contaminant mass and microbial diversity at a site with a complex pollution history. *J. Contam. Hydrol.* 144:1–19. <https://doi.org/10.1016/j.jconhyd.2012.10.009>.
- Rodríguez-Fernández, D., Torrentó, C., Guivernau, M., Viñas, M., Hunkeler, D., Soler, A., Domènech, C., Rosell, M., 2018a. Vitamin B<sub>12</sub> effects on chlorinated methanes-degrading microcosms: dual isotope and metabolically active microbial populations assessment. *Sci. Total Environ.* 621:1615–1625. <https://doi.org/10.1016/j.scitotenv.2017.10.067>.
- Rodríguez-Fernández, D., Heckel, B., Torrentó, C., Meyer, A., Elsner, M., Hunkeler, D., Soler, A., Rosell, M., Domènech, C., 2018b. Dual Element (C-Cl) Isotope Approach to Characterize Abiotic Reactions of Chlorinated Methanes by Fe(0) and by Fe(II) on Iron Minerals at Neutral and Alkaline pH. (Just accepted in *Chemosphere*).
- Shouakar-Stash, O., Frapé, S.K., Drimmie, R.J., 2003. Stable hydrogen, carbon and chlorine isotope measurements of selected chlorinated organic solvents. *J. Contam. Hydrol.* 60:211–228. [https://doi.org/10.1016/S0169-7722\(02\)00085-2](https://doi.org/10.1016/S0169-7722(02)00085-2).
- Tang, S., Edwards, E.A., 2013. Identification of *Dehalobacter* reductive dehalogenases that catalyze dechlorination of chloroform, 1,1,1-trichloroethane and 1,1-dichloroethane. *Philos. Trans. R. Soc. B* 368:20120318. <https://doi.org/10.1098/rstb.2012.0318>.
- Torrentó, C., Audí-Miró, C., Bordeleau, G., Marchesi, M., Rosell, M., Otero, N., Soler, A., 2014. The use of alkaline hydrolysis as a novel strategy for chloroform remediation: the feasibility of using construction wastes and evaluation of carbon isotopic fractionation. *Environ. Sci. Technol.* 48:1869–1877. <https://doi.org/10.1021/es403838t>.
- Torrentó, C., Palau, J., Rodríguez-Fernández, D., Heckel, B., Meyer, A., Domènech, C., Rosell, M., Soler, A., Elsner, M., Hunkeler, D., 2017. Carbon and chlorine isotope fractionation patterns associated with different engineered chloroform transformation reactions. *Environ. Sci. Technol.* 51:6174–6184. <https://doi.org/10.1021/acs.est.7b00679>.
- United states environmental protection agency (USEPA), 2014. Priority pollutants [WWW document]. <https://www.epa.gov/eg/toxic-and-priority-pollutants-under-clean-water-act>, Accessed date: 18 April 2017.
- Weathers, L.J., Parkin, G.F., 2000. Toxicity of chloroform biotransformation to methanogenic bacteria. *Environ. Sci. Technol.* 34:2764–2767. <https://doi.org/10.1021/es990948x>.
- Wiegert, C., Aeppli, C., Knowles, T., Holmstrand, H., Evershed, R., Pancost, R.D., Macháčková, J., Gustafsson, Ö., 2012. Dual carbon-chlorine stable isotope investigation of sources and fate of chlorinated ethenes in contaminated groundwater. *Environ. Sci. Technol.* 46:10918–10925. <https://doi.org/10.1021/es3016843>.
- Wiegert, C., Mandalakis, M., Knowles, T., Polymenakou, P.N., Aeppli, C., Macháčková, J., Holmstrand, H., Evershed, R.P., Pancost, R.D., Gustafsson, Ö., 2013. Carbon and chlorine isotope fractionation during microbial degradation of tetra- and trichloroethene. *Environ. Sci. Technol.* 47:6449–6456. <https://doi.org/10.1021/es305236y>.